Comprehensive studies on physical and chemical stability in liquid and glassy states of Telmisartan (TEL): Solubility advantages given by cryomilled and quenched material

Karolina Adrjanowicz, Marian Paluch, Kamil Kaminski, Lukasz Hawelek, Katarzyna Grzybowska, Daniel Zakowiecki

Comprehensive studies on physical and chemical stability in liquid and glassy states of Telmisartan (TEL): Solubility advantages given by cryomilled and quenched material

Journal:	*Philosophical Magazine & Philosophical Magazine Letters*
Manuscript ID:	TPHM-10-May-0175.R1
Journal Selection:	Philosophical Magazine
Date Submitted by the Author:	22-Jul-2010
Complete List of Authors:	Adrjanowicz, Karolina; University of Silesia, Institute of Physics Paluch, Marian; University of Silesia, Institute of Physics Kaminski, Kamil; University of Silesia, Institute of Physics Hawelek, Lukasz; University of Silesia, Institute of Physics Grzybowska, Katarzyna; University of Silesia, Institute of Physics Zakowiecki, Daniel; Pharmaceutical Works Polpharma SA, Preformulation Department R&D
Keywords:	amorphous materials, biological materials, dielectric materials, glass transition, glass
Keywords (user supplied):	

Comprehensive studies on physical and chemical stability in liquid and glassy states of Telmisartan (TEL): Solubility advantages given by cryomilled and quenched material

K. Adrjanowicz*, K. Grzybowska, K. Kaminski, L. Hawelek, M. Paluch

Institute of Physics, University of Silesia, Uniwersytecka 4, 40-007 Katowice, Poland

and

D. Zakowiecki

Preformulation Department R&D, Pharmaceutical Works Polpharma SA, Pelplinska 19, 83-200 Starogard Gdanski, Poland

Abstract

To make full use of the advantages given by amorphous pharmaceuticals it is necessary to understand the basic factors that determine their physical and chemical stability. Molecular mobility seems to be the most important one. Unfortunately, due to exceedingly long time scale required for molecular motion in the glassy state, direct monitoring of structural α-relaxation time (τ_α) in this temperature regime is rather difficult. The aim of current studies was to provide complete information about the time scale of α-mobility in glassy state of Telmisartan (TEL). For this drug a global molecular mobility seems to be the most dominant factor responsible for its long-term stability. Based on some estimation presented in our previous papers we concluded that at room temperature molecular mobility associated with the structural relaxation would exceed 3 years. Now, to characterize the temperature behavior of structural relaxation below glass temperature, T_g, we have used modified the Adam-Gibbs approach. Additionally, using results of dielectric measurements, we have performed a comparative analysis of molecular dynamics of amorphous TEL prepared by cryomilling as well as obtained by quench-cooling of the melt. The X-ray diffraction analysis was also carried out to confirm long-term stability of amorphous TEL, whereas solubility studies revealed its markedly better solubility profile than that for crystalline form. These findings have important implications for the further handling with this drug.

* Corresponding author e-mail: kadrjano@us.edu.pl

1. Introduction

Glasses have been well-known for thousands of years and now they constitute an essential group of materials. Amorphous ceramics, polymers or metals are commonly used in many fields of industry. Interestingly, during last 15 years amorphous materials have become considerably more attractive for food and pharmaceuticals scientists. Due to very specific physical properties of the amorphous phase, such materials typically have higher dissolution rate, solubility or even bioavailability, compared to crystalline counterparts [1, 2, 3]. Unfortunately, the glassy state is substantially less stable than the crystalline one. Because of that reason amorphous pharmaceuticals revert sooner or later to thermodynamically stable crystalline form, loosing in that way their key properties [4, 5, 6, 7]

Typically, amorphous pharmaceuticals are prepared using four different pathways. The first one, most conventional way based on a rapid cooling of a liquid. However, in some cases this method of amorphization cannot be employed, due to thermal degradation of many of drugs at theirs melting points. There are alternative ways of glass preparing such as amorphization from solutions (spray [8] and freeze drying [9]), from solid state (grinding [10] or pressurization of crystals [11]), compression of liquid [12] and by vapour deposition [13]. Recently among all non-conventional ways of amorphization cryogenic grinding has attracted a lot of attention. This method cannot be overestimated in case of many drugs, which undergo thermal degradation at melting temperature or have strong sensitivity to solvents. In the latter case a large problem might occurs while choosing the best solvents for freeze and spray drying techniques. However, it should be also noted that, physical stability of the amorphous drug prepared using various methods may differ significantly. As an example one can mention indomethacin. The glassy state of this drug obtained by very slow cooling of a liquid is stable against crystallization over 2 years, while the amorphous form obtained by cryogenic grinding is less stable and recrystallizes to 90% after approximately 13–15 h [14].

Ongoing studies have shown that among principal factors which affect crystallization from the amorphous state a special attention should be paid on the following issues: degree of molecular mobility, thermodynamic properties of the amorphous form, amount of water content (the presence of water favors crystallization) and the method of amorphization [14,15, 16, 17, 18]. However, to completely discuss the subject of physical stability of the amorphous drugs it is necessary to consider many other aspects, which also affect crystal nucleation and crystal growth rate. For example, it is well known that even various supercooling rates result in differences nucleation rate. In some cases a rapid and deep quenching is the only way of preparing some glasses, preventing from development of crystal nuclei. On the other hand,

fast cooling rate may cause additional strains that give rise to increase nucleation rate. Fukuoka et al [19] reported that glassy indomethacin reached by slow cooling from the melt revealed no tendency to crystallization at room temperature even after 2 years, while the quenched sample crystallize more rapidly.

Differences in re-crystallization properties of slowly and quench cooled samples were also reported by Yoshioka et at [5]. The dramatic impact on recrystallization of the amorphous state may also have even small amounts of chemical impurities, which can act as nucleation centers. It should be also noted that nucleation and the growth rate strongly depends also on the another very important factor, i.e. specific surface area (sample with larger surface area are generally less stable) and surface mobility [5, 14]. Yu et al [20,21] showed that surface-enhanced crystallization of glassy indomethacin and nifedipine can be even orders of magnitudes faster than bulk crystallization.

The vast majority of researchers and investigators dealing with pharmaceuticals admit that molecular mobility seems to be the key parameter affecting physical and chemical instability of the most amorphous drugs [22, 23, 24, 25]. It is also believed that long-term stability of those drugs can be obtained by storage at temperature where molecular mobility associated with structural relaxation time approaches to zero i.e at T_0 in Vogel-Fulcher-Tamman (VFT) equation [26]. This temperature was found to be close to so-called Kauzmann temperature, where entropies of supercooled liquid and crystal would be equaled [27]. For most of pharmaceuticals the storage temperature of 50 K below T_g is sufficient for the extension of the time scale of molecular motion to 3-5years of typical shelf-life. However, as shown for indomethacin the significant non-negligible mobility is detectable even 47 K below T_g [23]. Sometimes, it is also speculated that crystallization kinetics is not coupled with α-relaxation, but it is related to non-cooperative mobility associated with Johari-Goldstein secondary relaxation [28,29].

Anyway, because of the reasons given above it seems to be necessary to have some useful tool which enables us to probe α-relaxation times in the glassy state. The knowledge of the time scales of molecular motion below T_g is very important to verify whether alpha mobility at a certain storage temperature might cause a recrystallization of the amorphous drug or can be neglected as a factor of crystallization during typical shelf-life due to long α-relaxation times exceeding years. Obviously, because of practical reasons a direct determination of the structural relaxation time deep in the glassy state is not possible. However, there are some

combined theoretical and experimental means which enable us to evaluate the time scales of molecular motion below T_g.

To estimate the time scales of molecular motions in the glassy state one can use modified Adam-Gibbs-Vogel (AGV) equation proposed by Hodge [30], which is based on the nonlinear Adam-Gibbs equation

$$\tau_\alpha(T,T_f) = \tau_\infty \exp\left(\frac{DT_0}{T-(T/T_f)T_0}\right) \quad (1)$$

where τ_∞, D, T_0 are parameters from VFT equation used to fit the τ(T) dependence above T_g, T_f is so called fictive temperature that is an equilibrium temperature at which non equilibrium value of some macroscopic property would the equilibrium one.

The value of fictive temperature can be calculated from the configurational heat capacity ($C_p^{conf} = C_p^{liq} - C_p^{cryst}$) and the difference between heat capacity of liquid and glass ($C_p^{liq} - C_p^{glass}$) given as follows [31]

$$\frac{1}{T_f} = \frac{\gamma_{C_p}}{T_g} + \frac{1-\gamma_{C_p}}{T} \quad (2)$$

where

$$\gamma_{C_p} = \frac{C_p^{liq} - C_p^{glass}}{C_p^{liq} - C_p^{cryst}} \quad (3)$$

The values of heat capacities in above equation should be calculated at the glass transition temperature T_g. Parameter γ_{C_p} can vary from 0 to 1, indicating the temperature dependence of structural relaxation times of the real glass i.e. $\gamma_{C_p} = 1$ corresponds to Arrhenius behavior, while $\gamma_{C_p} = 0$ to VFT behavior below T_g. As it was demonstrated for several glasses, the value of γ_{C_p} is usually intermediate between those extremes (e.g. celecoxib $\gamma_{C_p} = 0.46$ [32], sorbitol $\gamma_{C_p} = 0.61$[31]). However, for indomethacin the Arrhenius-like dependence of structural relaxation times below T_g is expected ($\gamma_{C_p} = 0.92$) [22]. The AGV equation predicts in very simple and fast way a structural relaxation behavior at temperatures below T_g. However, it should be stressed that it was derived to describe non-equilibrium glassy dynamics. Consequently, it predicts correct structural relaxation times only for freshly prepared glass. With aging, structural relaxation times are expected to increase, approaching to values expected for equilibrium supercooled liquid [31].

Very recently Casalini and Roland (CR) have proposed a new method to determine τ_α in the glassy state [33]. This method takes advantage of the connection between the α-relaxation and the secondary β-relaxation of the Johari-Goldstein type and it simply based on monitoring changes of the β-relaxation with physical aging, which afterwards are used to characterize the structural relaxation dynamics in the glassy state. It is worth noting that for studied material, PVE, the values of aging time constant τ_{ag} turned out to be the same as τ_α calculated from the Coupling Model (CM) [34] and both of them were successfully use to follow the structural dynamics in the glassy state.

Encouraged by the success of this method, in our previous paper we have made an attempt to characterize in exactly the same way structural relaxation in the glassy state of pharmaceutical, Telmisartan (TEL) [35]. However, it should be pointed out that for TEL the values of τ_α^{CM} calculated from the CM substantially underestimates τ_{ag}, which can be explained by a large uncertainty in identifying the characteristic β-relaxation time for TEL due to its very broad maximum of the β-relaxation peak. Interestingly, good agreement between τ_{ag} from the aging experiment and those calculated from the CM we obtained only when dielectric data were analyzed in electric modulus representation [36]. Structural relaxation times τ_α in the glassy state were also evaluated by applying the time-temperature superposition (TTS) for the temperature region just below T_g i.e. selected α-relaxation peak, located just above T_g, was shifted horizontally to the temperatures below T_g so that its high-frequency side superimposes with the low-frequency side of spectra collected below T_g . Obtained in this way relaxation times $\tau_{\alpha-\mathrm{sup}}$ turned out to be in good agreement with that calculated based on aging experiment τ_{ag} . Our studies have revealed that molecular mobility associated with the structural relaxation at room temperature would exceed 3years and thus the α- mobility can be negligible in recrystallization of amorphous drug during its typical shelf-life. However, it doesn't mean that all molecular mobility become completely suppressed in that region i.e. local molecular motions associated with secondary relaxation JG-type (activation energy ~ 82kJ/mol) are still detectable [35].

The aim of present studies is to evaluate the structural relaxation times in the glassy state of TEL based on the AGV equation. For that purpose the thermal analysis of freshly prepared TEL glass were carried out. The temperature dependence of structural relaxation time below T_g obtained in this way was compared with prior results. Based on these results as well as the

X-ray diffraction patterns of amorphous TEL taken while one-year storage at room temperature, we would like to discuss about its long-term stability. Finally, we would like to also show what is the solubility advantage from amorphous TEL at different pH.

2. Experimental

2.1 Material

Telmisartan was supplied from Dr. Reddy's Laboratories Limited (India, CAS No 14470-48-4, purity ≥98%) and received as a white crystalline powder. Telmisartan is properly described chemically as 4'-[(1,4'-dimethyl-2'-propyl[2,6'-bi-1H-benzimidazol]-1'-yl)methyl]-[1,1'-biphenyl]-2-carboxylic acid. Its empirical formula is $C_{33}H_{30}N_4O_2$, its molecular weight is 514.63 g·mol^{-1}, and its chemical structure is presented in Fig. 1 [35]. Obtained material was used without further purification.

2.2 Methods

2.2.1 Methods of preparation amorphous TEL

Quenched sample - Crystalline TEL was placed on the stainless steel plate and then heated with use of hotplate until a complete melt was achieved. TEL was melted in air, during this procedure the temperature and sample color were carefully controlled. In the next step the sample was supercooled below T_g.

Cryomilled sample - Prior to milling crystalline sample was dried under vacuum at 313K for a period of 12hours. Total mass of sample was 2g. Grinding was performed using cryogenic impact mill (6750 freezer/mill SPEX CertiPrep, Inc., USA) consisting of a stainless steel vessel immersed in liquid nitrogen, within which a stainless steel rod is vibrated by means of magnetic coil. Before grinding 10 minutes of precool time was programmed. Then, the mill was planned to an impact frequency of 15 cycles per second for 6 min grinding periods separated by 3 min cool-down periods. The total milling time for our sample was 3hours. After milling, the grinding vial was immediately transferred to a vacuum oven and allowed to warm to room temperature. Freshly prepared cryomilled TEL is white powder. Before further investigation the water content was determined by the Karl Fischer (CRISON TitroMatic KF) method. For cryomilled TEL sample we have found 4% of water.

The amorphous form of quenched and cryomilled materials were checked by the X-ray powder diffraction method.

2.2.2 Thermogravimetric studies

The thermogravimetric measurement of the crystalline form of TEL was carried out with a Perkin Elmer TGA 1 thermal analyzer in a platinum measuring cell, with the use of Pyris

program for data handling. Measurements were performed in a nitrogen atmosphere with the heating rate 10K/min. The samples were heated up to 873K, starting from room temperature. Since we are not able to perform thermogravimetric measurements in air atmosphere, to check whether TEL melt without any degradation at this conditions we have used dielectric spectroscopy. TEL samples were melted in two different ways: in air and in nitrogen atmosphere, both were later quenched and dielectric measurements were carried out. By comparing at the same temperatures structural relaxation peaks and relaxation times we found no differences between samples melted in nitrogen and air. Hence, we expect that ably and carefully control melting procedure won't lead to thermal degradation of TEL even in air atmosphere.

2.2.3 Dielectric Spectroscopy

Isobaric dielectric measurements were carried out using a Novo-Control Alpha dielectric spectrometer (Novocontrol Technologies GmbH & Co. KG, Hundsangen, Germany). Our experiments were covered frequency range from 10^{-2} to 10^{7} Hz and temperature range from 133 to 463 K. The temperature was controlled using a nitrogen-gas cryostat with temperature stability better than 0.1 K. Cryomilled sample was placed between two stainless steel electrodes (diameter 20 mm) of the capacitor with a gap of 0.1 mm. The capacitor was made from a stainless steel. Dielectric spectra of cryomilled sample were collected in the temperature range from 193K to 453K. Above the glass transition temperature for cryomilled sample cold crystallization was recorded at 433K.

2.2.4 Differential scanning calorimetry (DSC)

DSC measurements were carried out using Perkin Elmer Pyris 1 DSC instrument (PerkinElmer Life And Analytical Sciences, Massachusetts, USA) with liquid nitrogen cooling. The instrument was calibrated for temperature and heat flow using high-purity standards of indium. Melting point was determined as the onset of the endothermic peak, whereas glass transition temperature as the midpoint of the heat capacity increment.

The sample (m=6.4mg) was placed in sealed aluminium pan. In the first scan thermograms were collected during heating of crystalline TEL at 10^{o}C/min from 360 to 560K (see Figure 6 in Results and Discussion Section). An endothermic, peak with an onset at 540K, identifies the melting of the sample at the temperature which agrees with that found in the literature (T_m=542±2K [37]). After melting, the sample was continuously cooled, achieving the glassy state without crystallization. In the second scan the subsequent heating from the glassy state was recorded, showing the characteristic signature for the glass transition in the heat capacity. At all temperatures the amorphous form of TEL has greater heat capacity C_p than that for crystal. The glass transition temperature (T_g=401K) was determined as the midpoint of the

heat capacity increment. This value agrees well with that calculated based on dielectric data (T_g=400K [35]).

2.2.5 Ultra-performance liquid chromatography (UPLC)

The chromatographic separation of TEL (crystalline and amorphous forms) and its impurities was achieved on the Waters Acquity UPLC system (Millford, MA, USA), equipped with reserved phase column, ACQUITY UPLC BEH C_{18} , 1.7 µm, 2.1 × 150 mm (Waters, Wexford, Ireland). Column temperature was maintained at 35° C. The ACQUITY UPLC system consisted of a Binary Solvent Manager, Sample Manager, Column Manager, and Photodiode Array eλ Detector (PDA). UV absorbance data were collected at 230 nm with a data collection rate of 40 points per second. The mobile phase consisted of a mixture of acetonitrile and purified water adjusted to pH 2.4 with ortho-phosphoric acid. The linear gradient program ran from 20% to 80% of acetonitrile over 15 minutes at a flow rate of 0.4 mL/min. The LC separation was achieved within runtime of 11 minutes; therefore the chromatograms were recorded within this time. Chromatographic data were acquired and calculated using the Empower Pro 2 software (Waters, Millford, MA, USA). The method was used for determination of related substance of TEL, as well as in solubility of the active pharmaceutical ingredient study.

2.2.6 Solubility studies

The solubility of different forms of TEL was determined in different medias such as purified water, hydrochloric acid (0.1 M), acetate buffer pH 4.5, phosphate buffers pH 4.5, 6.8 and 7.5 (Table II). Solubility measurement was performed at specific pH values using shake-flask method at 37°C ± 0.5°C.

3 Results and discussion

3.1 Test of thermal stability of TEL

Accordingly to the information found in the literature TEL has relatively high melting temperature (T_m around 542K [37]), compared to other pharmaceuticals being under our consideration previously (e.g. indomethacin T_m=434K [12], ibuprofen T_m= 348K [38], verapamil hydrochloride T_m=421K [39]). It is also well-known that there is a great number of drugs which crystalline forms are thermally unstable or melt with decomposition (e.g. diuretic agents [40]). Consequently, in such compounds the glassy state cannot be obtained by supercooling the melt. Unfortunately, in the literature it was difficult to find any information about the extent of thermal stability studied herein pharmaceutical. Thus, we have performed additional thermogravimetric measurements in order to test if the examined drug undergoes thermal degradation at T_m. The thermogravimetric and derivative curves are shown in Fig. 1.

As can be seen TEL is thermally stable up to 587K. At this temperature a thermal decomposition of the sample begins and is nearly complete at about 773K (mass loss 77%), giving a final residue of less than 20%.The sample is decomposed in a single weight loss. This is supported by the derivative curve which exhibits only a single peak (Fig. 1 inset).

3.2 UPLC studies on chemical stability of amorphous TEL samples obtained by quenching and cryomilling.

For drug manufacturers it is well- known that before each substance can be placed on the market it must satisfy increasingly rigorous regulations, like the highest purity standards. Thus, every drug substance or drug product should be free of any impurities or degradation products, which amount can also increase during the shelf-life. Thus, using ultra performance liquid chromatography (UPLC) we have analyzed crystalline as well as amorphous TEL samples in order to provide additional information about their purity. The UPLC is one of the main analytical techniques used for controlling the quality or consistency of active substances and final dosage forms [41,42]. It is also well-established and reliable source of information whether any decomposition of chemical entities occur [e.g.43].

The chromatogram of crystalline TEL was used for further analysis as a reference. As displayed in Fig. 2 (a) it consists of one very well pronounced peak with the retention time 7.5 min, ascribed to TEL and two others very small with the retention times 5.6 and 6.5 min, respectively. The analysis of area under the peak assigned to the TEL is equal to 99.96% while the total sum of impurities doesn't exceed more than 0.04%. This confirms that the initial crystalline material has high purity. The UPLC chromatograms of amorphous TEL obtained by cryomilling and quenching are presented in Figure 2 panels (b) and (c), respectively. In both cases, it is clearly visible that the main peak ascribed to TEL drug has exactly the same retention time as that observed for crystalline one. However, during amorphization of TEL by cryomilling as well as quenching few impurities were formed. Comparison of impurities profile of different forms of TEL is presented in Table I. When one looks carefully it is visible that that the amount of imp.3 and imp.6 (detectable even in crystalline TEL) increased for cryomilled and quenched samples. Significant increment of the amount of unknown impurity 01 (with relative retention time 0.17min) and unknown impurity 09 (with relative retention time 1.31min) was also observed. These results suggest that that during amorphization by both the methods impurities are formed by degradation on insignificant level, with no consequences to the physical, chemical and pharmacokinetic properties of amorphous TEL. Although the purity drop of amorphous TEL due to processing was recorded, our samples certainly do not exceed threshold for impurities acceptable by

modern pharmacy and are highly pure (>99%). Few years ago, Savolainen et al [44] showed that theirs samples: slow/quench cooled and milled indomethacin had degraded due to manufacturing process about 3% and 0.5%, respectively. In view of all these findings, appearance of unwanted impurities is unavoidable event occurring during conversion of pharmaceutical into amorphous form.

3.3 Analysis of molecular dynamics in cryomilled TEL

Dielectric loss spectra of cryomilled TEL were measured below and above its glass transition temperature T_g, starting from heating amorphous cryomilled TEL from the room temperature to the region above the T_g. Representative spectra are shown in Figure 3(a). Similarly to the ordinary glass obtained by supercooling of melt (these spectra can be found in our previous paper [35]), below T_g a well defined β-peak appears below T_g. However, in contrast to previously measured sample, in cryomilled TEL another faster relaxation mode appears. We have designated this process as ν-relaxation. Additional studies, based on Karl Fisher method have proven that the ν-relaxation is an effect of the presence of the water in investigated sample (in our system we have about 4% of water fraction). This finding indicates that even small amount of water being present in cryomilled material significantly changes the relaxation dynamics of amorphous TEL and causes the appearing of a new additional mode in the dielectric loss spectra below T_g. The ν process originating from motions of water molecules has the same temperature sensitivity, as secondary relaxation in many glass-forming liquids [45]. This can be seen in Figure 3(b) where ν-relaxation peak moves towards lower frequencies with decreasing temperature. It is worth noting that with increasing temperature the ν-relaxation becomes hardly visible and by approaching boiling temperature of water it is completely imperceptible. Then, the positions as well as the shape of β-relaxation process are identical to those for quenched TEL (Figure 3(c)). It is worth noting that when the cryomilled sample was heated to 433K, kept at this temperature for about 1h and then quenched in order to its re-amorphization, the presence of the ν-relaxation reflecting water molecules dynamics was not detected in the loss spectra. This happens since all water evaporated from the sample at higher temperatures.

In Figure 4(a) we present dielectric loss spectra of cryomilled TEL collected above its glass transition temperature. Analogously as for a quenched sample the dc-conductivity has been subtracted from the measured dielectric spectra. As can be seen the structural relaxation peak appears exactly in the same temperature region as for quenched sample. Subsequent heating of cryomilled TEL leads to cold crystallization process, which is visible in dielectric loss

spectra as a decrease of intensity of structural relaxation process at about T=433K. From inspection of the spectra shapes and positions of the α-process above T_g's in quenched and cryomilled TEL we found out that there are practically the same. As shown in the main part of Figure 4(b) the structural relaxation obtained for cryomilled material is slightly shifted toward the higher frequencies. However, the shape of the α-peak is invariable (see Fig. 4(b) inset).

From dielectric loss spectra, we get the relaxation map for cryomilled TEL. It is presented in Figure 4(c) together with dielectric data for quenched sample. The α, β and ν-relaxation times were determined as an inverse of the frequency of the maximum peak position ($\tau=(2\pi f_{max})^{-1}$). The temperature dependence of α-relaxation time is well-described by the VFT equation. Here, followed by the common rule we defined the glass transition temperature as a temperature at which dielectric relaxation time τ_α is equal to 100 seconds. For cryomilled TEL T_g was found to be equal 401K, which is in satisfactory agreement with that reported for quenched one (T_g=400K [35]). In amorphous cryomilled TEL the temperature dependences of the β and ν-relaxation times exhibit a linear dependence and can be well-described by Arrhenius power-law (see Fig.4(c))

$$\tau_\beta = \tau_\infty \exp\left(\frac{E_\beta}{k_B T}\right) \qquad (4)$$

with $\log_{10}\tau_\infty = -15.6 \pm 0.8 s$, E_β=81.7±4kJ/mol for the β-relaxation and $\log_{10}\tau_\infty = -13.9 \pm 0.2 s$, E_ν=48±1kJ/mol for the ν-relaxation. The value of activation energy for the β-process found in this studies agrees very well with that reported for quenched TEL sample (E_β=81.8kJ/mol [35]). Hence, we get that irrespective of amorphization way the β-relaxation (identify by us as Johari-Goldstein process [46,47]) shows the same behaviour. The value of energy barrier found for relaxation of water molecules (ν-process) is close to that found for water in confined systems (E_ν=44.4±3.7kJ/mol [48]).

Concluding this part, we have shown that amorphous TEL obtained by milling at liquid nitrogen temperature revealed additional secondary relaxation process (faster one), not reported in case of quenched sample. This process describes relaxation dynamics of water molecules. Its presence in cryomilled TEL simply reflects substantial difficulty associated with controlling the water uptake while handling with freshly cryogrinded powder. It also highlights the extremely high tendency of amorphous materials to absorb a significant amount of water vapor from surroundings. In our case we found that cryomilled TEL absorbed about 4% of water. Despite that it should be also emphasized that independent of amorphization

method the temperature behavior of β-relaxation seems to fall under same pattern of behavior and take source from the same intermolecular mobility. For TEL, we also found that the shapes and positions of structural relaxation peaks are essentially the same, leading to practically identical glass transition temperatures. Herein, we would like to refer to our latest paper concerning another pharmaceutical, glibenclamide (GMC), where in the glassy state secondary relaxation of intramolecular origin was detected [49]. What is interesting to note, cryomilling and quenching of GMC lead to the same temperature behavior of the γ-relaxation process (same activation energies for the γ-process were found) and just slight difference in the glass transition temperatures was observed. However, this discrepancy in the glass transition temperatures can be explained due to tautomerisation phenomena. Nevertheless, in the literature an opposite behavior was also noted. For example, Decamps et al reported that molecular mobility below T_g of trehalose strongly depends on the method how the amorphous sample was prepared [50].

3.4. Prediction of the temperature behavior of structural relaxation process in amorphous TEL based on Modified Adam-Gibbs Approach.

Figure 5 shows the temperature dependences of structural relaxation times for TEL in supercooled and glassy state. These data are taken from our previous paper [35]. The temperature dependence of τ_α in supercooled state (blue triangles) was experimentally measured, while the τ_α behaviors in the glassy state were estimated using various approaches i.e. from aging experiments τ_{ag} (red solid squares), the Coupling Model (green open triangles) and by applying time-temperature superposition (TTS) for the temperature region just below T_g , τ_{sup} (yellow solid circles). As can be seen, in supercooled state the temperature behavior of structural relaxation times follows simple VFT equation. This situation firmly changed below T_g, where the $\tau_\alpha(T)$ dependence does not follow any more that from the region above T_g. Now, it is of interest to investigate how the modified Adam-Gibbs model describes molecular dynamics in glassy state of TEL, and if there is consistency between relaxation times evaluated from Eq. (1) and those previously determined.

In the first step, using the modified Adam-Gibbs approach we have generated the curve, which describes relaxation times τ_{ag} as well as τ_{sup} in the most satisfactory way. In Figure 5, this curve can be seen as a blue solid line, with $\gamma_{C_p} = 0.91$. As the values of parameters τ_∞, D, T_0 in Eq. (1) we have used those from VFT equation fitted to the $\tau(T)$ dependence in the supercooled liquid state. The same procedure we have also applied to fit structural relaxation

Formatted: Superscript
Deleted: 35

in the glassy state predicted from the CM, τ_α^{CM}. This curve is seen in Figure 5 as a green dotted line, with $\gamma_{C_p} = 1$. If theoretically the VFT equation were valid also in the temperature region below T_g, it should give the other limited value - $\gamma_{C_p} = 0$ (extended VFT solid black line visible in Figure 5). Values of γ_{C_p} are very often used to characterize the temperature dependence of relaxation times ('fragility') in the glassy regime [31,51]. Hence, we obtain that for glassy TEL more Arrhenius-type (or rather 'strong') behavior is expected if relaxation times in the glassy state really follow the τ_{ag} and τ_{sup} dependences. On the other hand, when we assume that the correlation between α-relaxation and JG process persists also in the glassy state (τ_α^{CM}), we may expect then typical Arrhenius-type (strong) behavior of structural relaxation time below T_g.

In the next step, molecular mobility in non-equilibrated, freshly formed glassy state of TEL was determined as a function of temperature using AGV equation (eq. 1), with the fictive temperature estimated based on calorimetric measurements. In order to calculate the value of γ_{C_p} DSC studies were carried our (the heat capacity measurements are carefully described in experimental section). In Figure 6 we present the heat capacity data used to determine γ_{C_p}. For TEL we obtained the following values of heat capacities at T_g: $C_p^{liq} = 1.92 J/gK$, $C_p^{cryst} = 1.4 J/gK$ and $C_p^{glass} = 1.53 J/gK$. Thus, the heat capacity step at the glass transition is $\Delta C_p = C_p^{liq} - C_p^{liq} = 0.39 J/gK$. This value is rather moderate one, when we compared with other pharmaceutical systems e.g. indomethacin $\Delta C_p = 0.41 J/gK$ [51], glibenclamide $\Delta C_p = 0.45 J/gK$ [1], or ibuprofen $\Delta C_p = 0.37 J/gK$ [52]. Since the heat capacity step gives information about number of accessible molecular conformation at T_g, it was suggested that it might be very useful to predict the ease of crystallization. As shown for few pharmaceuticals the increase of ΔC_p at T_g leads to more stable glass. For example, celecoxib with $\Delta C_p = 0.26 J/gK$ was found to have significant crystallization abilities above as well as below T_g, while ritonavir ($\Delta C_p = 0.55 J/gK$) does not exhibit any tendency to crystallization. [32]. However, while predicting degree of molecular mobility in the glassy state by means of thermal analysis, one should bear in mind that the heat profile depends on temperature as well as time and it might be completely different for amorphous samples obtained using various methods. For TEL, based on heat capacity measurements of quenched sample, we found

γ_{C_p} to be 0.75±0.07. This value was used afterwards to obtain the fictive temperature (Eq.2) and the structural relaxation behavior in the glassy state (Eq. 1). Calculated relaxation times as a function of temperature are shown in Figure 5 as red dash-dotted line. One can see that relaxation behavior evaluated based on direct thermal analysis undergo larger changes with temperature than the relaxation curve generated for aging experiments and TTS data. Consequently, predicted α-relaxation time behavior becomes even more fragile. Substantial discrepancy between α-relaxation times in the glassy state of TEL determined through a specific heat analysis and relaxation times already known is evident. Here, it should be also pointed out that significant limitation of modified Adam-Gibbs method is that it predicts same molecular mobility for glasses prepared using various methods and having different thermal histories. However, as shown in the literature, the time scales of molecular motion below T_g might strongly depend on the experimental conditions [53].

Regarding to the modified Adam-Gibbs approach, it is appropriate for predicting molecular dynamics in non-equilibrium glasses. Thus, when we calculate $\gamma_{C_p} = 0.75$ based directly on heat capacities analysis, the evaluated structural relaxation behavior in the glassy state concern only freshly formed non-equilibrium sample. On the other hand relaxation dynamics with the value of $\gamma_{C_p} = 0.91$ was generated for glass having different thermal history and being in completely different position with respect to their equilibrium values. Moreover, during aging at fixed temperature we have followed time evolution of β-relaxation based on assumption that it follows α-relaxation changes towards equilibrated value, despite that the τ_{ag} values don't necessary represent completely equilibrated relaxation times τ_α. Consequently, they don't present relaxation dynamics of glass preparing in exactly the same way, having identical thermal history but various dynamics of two different non-equilibrated systems. Because of reasons given above, it is rather difficult to make descriptive comparison between degree of molecular mobility predicted from AGV equation and other approaches.

As we have mentioned previously, the knowledge of structural relaxation behavior in the amorphous state, that is whether it is being more Arrhenius or VFT- like, is very important for pharmaceutical scientists in order to find appropriate storage conditions (preventing from crystallization) as well as further dealing with glassy drugs. It concern especially amorphous materials in which crystallization tendency is related mainly to the α-mobility. As can be seen in Figure 5, for a system which structural relaxation times below T_g follows Arrhenius-like behavior the typical shelf-life time is reached at vastly lower temperature, far from glass

transition temperature. For TEL (T_g=400K) even if we assume that the structural relaxation dynamics below T_g follows τ_α^{CM} the time scale of molecular motion at room temperature and even human body temperature, should exceed 3-years. Because of that reason, amorphous TEL is certainly being the best candidate for further pharmaceutical investigations.

3.5. Experimental verification of physical stability of amorphous TEL

Study of molecular mobility in glassy state is important for predicting storage stability.

Based on structural relaxation behavior below T_g predicted by means of AGV equation as well as relaxation times τ_{ag} evaluated previously by following the β-relaxation changes while aging experiment, we have pointed out that structural relaxation time of TEL at room temperature would exceed 3 years. As a consequence, if α-mobility mostly controls crystallization from the amorphous state, it should maintain physically stable during typical shelf-life. Anyway, we have also noticed that some local molecular mobility (β-relaxation) is still detectable at this temperature region and in accordance with information found in the literature this type of motion should be also taken into account.

Now, we would like to present experimental verification of theoretically predicted long-term stability of amorphous TEL. To confirm amorphous nature of our quenched and cryomilled samples we have carried out repeatedly the X-ray powder diffraction (XRD) measurements. The XRD patterns were recorded every month for up to 1 year. In Figure 7 (a) we present diffraction pattern for crystalline TEL (given here as a reference one), while the XRD patterns for cryomilled and quenched samples taken respectively after 8 and 14 months of storage at room temperature are shown in Figure 7(b) and 7(c).Very broad peaks observe therein, compared to sharp Bragg peaks typical for crystalline state, indicate that examined materials are so far completely amorphous. Interestingly, both samples remain physically stable irrespective of storage conditions i.e. whether there is constant air access or not (corresponding figures not shown in this paper). This is very important finding, since it is well-known that significant amount of water vapor by glass from surroundings may result in its physical instability. Taking into account presented above results we can conclude that physical stability of amorphous TEL at room temperature is related to its lower alpha molecular mobility rather than the β-mobility. Most probably it also doesn't depend on method of amorphization and humidity conditions.

3.6 Analysis of crystallization kinetics in supercooled liquid TEL

Since the degree of molecular mobility seems to play a key role in crystallization tendency of many amorphous pharmaceuticals, the relationship between physical instability and structural

relaxation process has received a great interest. In this part, we have studied crystallization kinetics of TEL above its glass transition temperature in order to draw appropriate correlation between molecular mobility and crystallization rate below T_g. Amorphous TEL, obtained by quenching as well as cryogrinding, was found to crystallize above its glass transition temperature, while no crystallization event was reported below the T_g (this point was carefully discussed in the previous part of this paper). A subsequent heating of amorphous TEL leads to re-crystallization event occurring above 453K and proceeds at considerable rate (see Fig 4(a)). To obtain detailed information about isothermal crystallization profile of TEL we have prepared time-depending dielectric measurements above its glass transition temperature. It is worth to mention that dielectric spectroscopy is one of the most suitable technique employed to study crystallization kinetics in many systems having non-zero value of its dipole moment [e.g. [52], [54]]. The crystallization process can be followed directly in the real (ε') and imaginary part (ε") of complex dielectric permittivity. In the real part of complex dielectric permittivity this situation is reflected by decrease of static permittivity increment (Figure 8(a)), while in imaginary part by decrease intensity of the structural relaxation peak. (Figure 8(b)). However, before crystallization process begin the changes in dielectric response were not been observed for appropriately t_0=1200s. This time, so called 'induction time' is required for molecular mobility to rearrange and take appropriate position so that crystallization process can occur. It is interesting to note that with crystallization progress the shape and position of α-peak practically don't change, no additional relaxation processes emergence. However, at final stages of crystallization large electrode polarization effect in dielectric loss spectra occurs. As can be seen in Figure 9(a) crystallization progress is manifested by drastic drop of dielectric strength $\Delta\varepsilon$ of the structural relaxation process due to decreasing number of reorientationing dipoles (accordingly with $\Delta\varepsilon \propto n\mu^2$). When 100% crystallinity is achieved dielectric strength should present a zero value.

The progress of crystallization is usually followed by the normalized dielectric constant given as follows [[55],[56]]

$$\varepsilon'_N(t) = \frac{\varepsilon'(0) - \varepsilon'(t)}{\varepsilon'(0) - \varepsilon'(\infty)} \quad (5)$$

where $\varepsilon'(0)$ is dielectric constant at the beginning of crystallization, $\varepsilon'(\infty)$ is the long time limiting value of dielectric constant, and $\varepsilon'(t)$ is the value at time t. Obtained in this way normalized curve plotted versus time is presented in Fig 9(b).

Crystallization kinetics of studied herein sample follows Avrami equation [[57]]

$$\varepsilon'_N(t) = 1 - \exp[-kt^n] \quad (6)$$

with rate constant $k = 1.4 \times 10^{-8} s$ and Avrami exponent $n = 2$. The value of n=2 indicates athermal nucleation followed by two-dimensional crystal.

Finally, the crystallization half-time, defined as a time at which the crystallinity reached 50% of the maximum crystallinity, was found to be $t_{1/2}$=2.5h. It is worth to note, that at this temperature crystallization time is considerably longer than time required for molecules to reorientate (structural relaxation time $\tau_\alpha \approx 1 \times 10^{-5} s$). The fact that structural relaxation is fairly faster in supercooled and liquid state than crystallization process is a common feature of many systems. On the contrary in the glassy state this behavior might be completely different. For many amorphous pharmaceuticals it was reported that crystallization rate is comparable or even faster than structural relaxation [58]. Unfortunately, the mechanism of crystallization from the glassy state is till now not fully understand and remain an open issue. However, if we assume that crystallization mechanism won't significantly change while passing liquid-glass transition and in the glassy state it is still mostly governed by α-mobility that would explain experimentally measured its long-term stability of at room temperature.

3.7. Solubility measurements

As a final point we would like to present results of solubility measurements of crystalline and amorphous form of TEL (cryomilled and quenched). During determination of solubility it was found the differences between both forms as well as between cryomilled material and quenched TEL (see Table 2). During solubility studies of amorphous substances, no re-crystallization process was observed. Solubility of TEL was found to be decrease with the pH of medium. The saturation solubility of the drug was maximal in acidic conditions (0.1 M HCl). Taking under consideration form of telmisartan it was observed significantly greater solubility of amorphous telmisartan than crystalline form. Comparing two amorphous form of active pharmaceutical ingredient, telmisartan quenched, in majority media, showed better solubility than cryomilled substance (Fig. 10 as well as Table 2).

4. Conclusions

The knowledge of the time scales of molecular motion in the real glass is of great interest many researchers dealing with amorphous pharmaceuticals. Unfortunately, this region is experimentally inaccessible for α-mobility. Consequently, to evaluate degree of molecular motion below T_g theoretical approaches have to be used. In our previous paper we have made an attempt to predict structural relaxation times in the glassy state of TEL based on Casalini and Roland approach as well as the Coupling Model. As a result we get that the structural

relaxation time exceed 3 years at room temperature, which should guarantee long-term stability of amorphous TEL. In this work, we present results obtained by means of modified Adam-Gibbs method for a freshly formed glass. Although, the difference between structural relaxation times calculated from AGV equation and those previously determined is evident, it can be reasonable explain by different thermal histories of samples. These results suggest that prediction of molecular dynamics reflected in the structural relaxation in the glassy state is more complex. It depends on many circumstances and cannot be generalized for all amorphous materials obtained using various routes.

We have also studies molecular dynamics in cryomilled TEL in order to find if there is any difference when compare to glass obtained by quenching. Below T_g, we observed additional secondary relaxation process, not reported for quenched sample. However, as we get this relaxation process can be ascribed to relaxation of water molecules, since cryomilled TEL sorbed about 4% of water from the surroundings. It is remarkable that quenched TEL remain amorphous even after 1 year of storage at room temperature. This result indicates that long-term stability of TEL is mostly caused by extremely slow α-mobility, not by much faster, still detectible at room temperature β-mobility.

Finally, we have also checked what the experimental solubility gain given by amorphous form of TEL, showing a considerable improvement of drug solubility. The biggest difference is observed for low pH solutions. Our studies revealed that solubility of amorphous TEL obtained using various methods of amorphization (i.e quenching and cryogrinding) are not the same. Comparing those two amorphous forms we get that quenched sample, in majority medias, showed better solubility than cryomilled substance. Experimentally verified long-term stability of amorphous TEL as well as its favorable solubility properties makes it potentially very attractive for further biopharmaceutical consideration.

Acknowledgments

The authors (KA, KG, KK, MP) deeply thankful for the financial support within the framework of the project entitled /From Study of Molecular Dynamics in Amorphous Medicines at Ambient and Elevated Pressure to Novel Applications in Pharmacy/, which is operated within the Foundation for Polish Science Team Programme co financed by the EU European Regional Development Fund.

References

[1] B. C. Hancock, M. Parks, Pharm. Res. 17 (2000) 397-404

[2] D. Craig, P. Royall, V. Kett, M. Hoptopn, Int. J. Pharm. 179 (1999) 179-207

[3] M. Mosharraf, C. Nystrom, Pharm. Sci. (1998) 1, S268

[4] P. Gupta, A. K., AAPS PharmSciTech 6 (2005) Article 32

[5] M. Yoshioka, B. C. Hancock, G. Zografi, J. Pharm. Sci. 83 (1994) 1700

[6] A. Saleki-Gerhardt, G. Zografi, Pharm. Res. 11 (1994) 1166-1173

[7] D. Zhou, G. Geoff, Z. Zhang, D. Law, D. Grant, E.A. Schmitt, Mol. Pharmaceuticals, 5 (2008) 927-936

[8] O. I. Corrigan, E. M. Holohan, K. Sabra, Int. J. Pharm. 18 (1984) 195–200

[9] L. Chang, D. Shepherd, J. Sun, D. Ouellette, K. L. Grant, X. Tang, M. J. Pikal, J. Pharm. Sci 94 (2005) 1427–1444.

[10] S. Qi, I. Weuts, S. Cort, S. Stokbroekx, R. Leemans, M. Reading, P. Belton, D. Q. M. Craig, J. Pharm. Sci., 99 (2010) 196-208

[11] A. Hedoux , Y. Guinet, F. Capet, L. Paccou, M. Decamps, Phys. Rev. B 77 (2008). 094205

[12] Z. Wojnarowska, K. Adrjanowicz, P. Wlodarczyk, E. Kaminska, K, Kaminski, K. Grzybowska, R. Wrzalik, M. Paluch, K.L. Ngai, J Phys. Chem. B 113 (2009) 12536

[13] K. J. Dawsona, K. L. Kearnsa, Lian Yub, W. Steffenc, M. D. Ediger, PNAS, 106 (2009) 15165-15170

[14] K. Crowley, G. Zografi, J. Pharm. Sci. 91 (2002) 492 - 507

[15] C. Bhugra,R. Shmeis, M. J. Pikal, J. Pharm. Sci. 97 (2008) 4446-4458

[16] C. Bhugra, M. Pikal, J. Pharm. Sci, 97 (2007) 1329–1349

[17] V. Andronis, M. Yoshioka, G. Zografi. J. Pharm. Sci. 86 (1997) 346–351

[18] V. Andronis, M. Yoshioka, G. Zografi, J. Pharm. Sci. 86 (1997) 346-351

[19] E. Fukuoka, M. Makita, S. Yamamura, Chem. Pharm. Bull. 34 (1986) 4314.

[20] T. Wu and L. Yu, Pharm. Res. 23 (2006) 2350-2355

[21] L. Zhy, L. Wong, L. Yu Mol. Pharm. 5 (2008) 921-926

[22] V. Andronis, G. Zografi, Pharm. Res. 15 (1998) 835–842

[23] B. C. Hancock, S. L. Shamblin, G. Zografi, Pharm. Res. 12 (1995) 799-806

[24] S. L. Shamblin, B. C. Hancock, M. J. Pikal, Pharm. Res. 23 (2006) 2254-2268

[25] S. Yoshioka, Y. Aso, J. Pharm. Sci. 96 (2007) 960-981

[26] H. Vogel, Physikalische Zeitschrift 22 (1921) 645-6, G. Fulcher, J. Am. Cer. Soc. 8 (1925) 339 – 355, G. Tammann, W. HesseGöttingen, Zeitschrift für anorganische und allgemeine Chemie, 156 (1926) 245 – 257

[27] W. Kauzmann, Chem. Rev. 43 (1948) 219–256

[28] T. Hikima, T. Hanaya, M.Oguni, J. Non-Cryst. Solids, 235-237 (1998) 539-547

[29] J. Alie, J. Menegotto, P. Cardon, H. Duplaa, A. Caron, C. Lacabanne, M. Bauer, J. Pharm. Sci. 93(2004) 218

[30] I.M. Hodge, Macromolecules 20 (1987) 2897

[31] S. L. Shamblin, X. Tang, L. Chang, B. C. Hancock, M. J. Pikal, J. Phys. Chem. B. 20 (1999) 4113-4121

[32] P. Gupta, G. Chwala, A. K. Bansal, Mol. Pharm, 1 (2004) 406-413

[33] R. Casalini, C. M. Roland, Phys. Rev. Letters 102, 035701 (2009)

[34] K. L. Ngai, R. W. Rendell, Supercooled Liquids, Advances and Novel Applications (ACS Symposium Series 1997 vol 676) ed J T Fourkas, D Kivelson, U Mohanty and K Nelson (Washington, DC: American Chemical Society) chapter 4, p. 45 (1997)

[35] K. Adrjanowicz, Z. Wojnarowska, P. Wlodarczyk, K. Kaminski, M. Paluch, J. Mazgalski, Eur. J. Pharm. Sci. 38 (2009) 395–404

[36] K. Adrjanowicz, M. Paluch, K. L. Ngai, J. Phys.: Condens. Matter 22 (2010) 125902

[37] H. Schneider, United States Patent No. 6358986 (2002)

[38] K. Adrjanowicz, K. Kaminski, Z. Wojnarowska, M. Dulski, L. Hawelek, S. Pawlus, M. Paluch, W. Sawicki, J. Phys. Chem. B. (2010)

[39] K.Adrjanowicz, K. Kaminski, M. Paluch, P. Wlodarczyk, K. Grzybowska, Z. Wojnarowska, L. Hawelek, W. Sawicki, P. Lepek, R. Lunio, J. Pharm. Sci. 99 (2010) 828-839

[40] D. M. S. Valladao, L. C. S. De Oliveira, J. Zuanon Netto, M. Ionashiro, J. Therm. Analysis, 46 (1996) 1291-1299

[41] L. Novakova, L. Matysova, P. Solich, Talanta 68 (2006) 908-918.

[42] S. A. C. Wren, P. Tchelitcheff, J. Chromatogr. A 1119 (2006) 140-146.

[43] R.Toporisic, A. Mlakar, J.Hvala, I. Prislan, L. Z. Kralj, J.Pharm. Biomed. Analysis 52 (2009) 294-299

[44] M. Savolainen, A. Heinz, C. Strachan, K. Gordon, J. Yliruusi, T. Rades, N. Sandler, Europ. J. Pharm. Sci. 30 (2007) 113-123

[45] S. Capaccioli, K. L. Ngai, N. Shinyashiki, J. Phys. Chem. B, 111 (2007) 8197–8209

[46] G. P. Johari, M. Goldstein, R. Simba, Annu. New York Acad.Sci. 279 (1976) 117

[47] G. P. Johari, M. Goldstein, J. Chem. Phys. 55 (1971) 4245

[48] S. Cerveny, G. A. Schwartz, R. Bergman, J. Swenson, Phys. Rev. Lett. **93**, 245702 (2004)

[49] Z. Wojnarowska, K. Grzybowska, K. Adrjanowicz, K. Kaminski, M. Paluch, L. Hawelek et al., "Study of the amorphous glibenclamide drug: Analysis of the molecular dynamics of quenched and cryomilled material", Mol. Pharm. (2010) In press.

[50]

[51] K. J. Crowley, G. Zografi, Thermochemica Acta 380 (2001) 79-93

[52] A.R. Brás, J. P. Noronha, A. M. Antunes, M.M. Cardoso, A. Schönhals, F. Affouard, M. Dionísio, N. T. Correia, J. Phys. Chem. B, 112 (2008) 11087-99

[53] J. D. Stevenson, P. G. Wolynes, J. Phys. Chem. B, 109 (2005) 15093-15097

[54] G. T. Rengarajan, M. Beiner, Letters in Drug Design & Discovery, 3 (2006) 723-730

[55] S. Napolitano, M. Wübbenhorst, J. Non. Cryst. Solids, 353 (2007) 4357-4361

[56] M. T. Viciosa, N. T. Correia, S. M. Salmerón, A. L. Carvalho, M. J. Romão, J. L. Gómez Ribelles, M. Dionísio, J Phys Chem B. 113 (2009)14209-17.

[57] M. Avrami, J. Chem. Phys., 17 (1939)pg. 1103

[58] D. Zhou, G. G. Z. Zhang, D. Law, D. J. W. Grant, E. A. Schmitt, Mol. Pharm. 6 (2008) 927-936

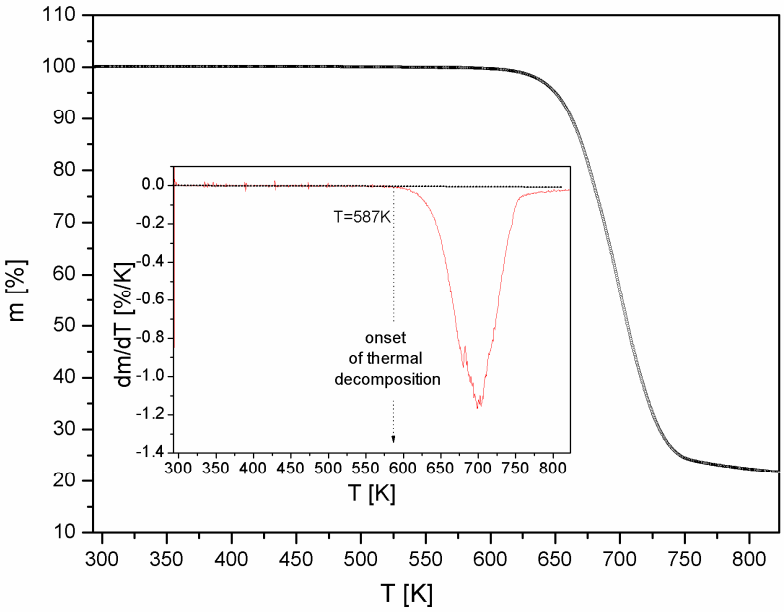

Figure 1. Thermogravimetric curve weight loss curve (main part of the plot) and derivative weight loss curve (inset) of crystalline TEL.

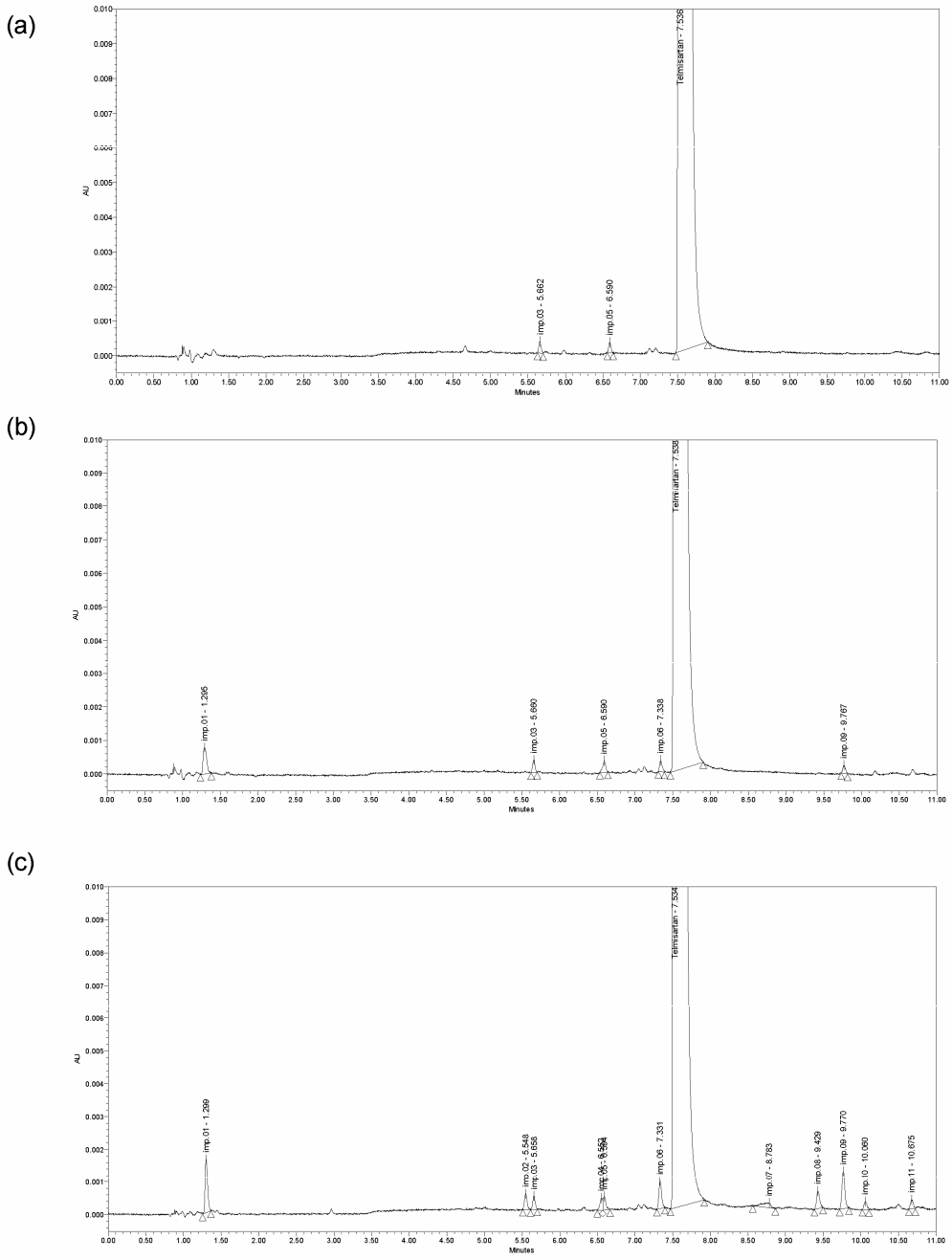

Figure 2. Typical chromatogram of TEL (a) crystalline, (b) cryomilled and (c) quenched

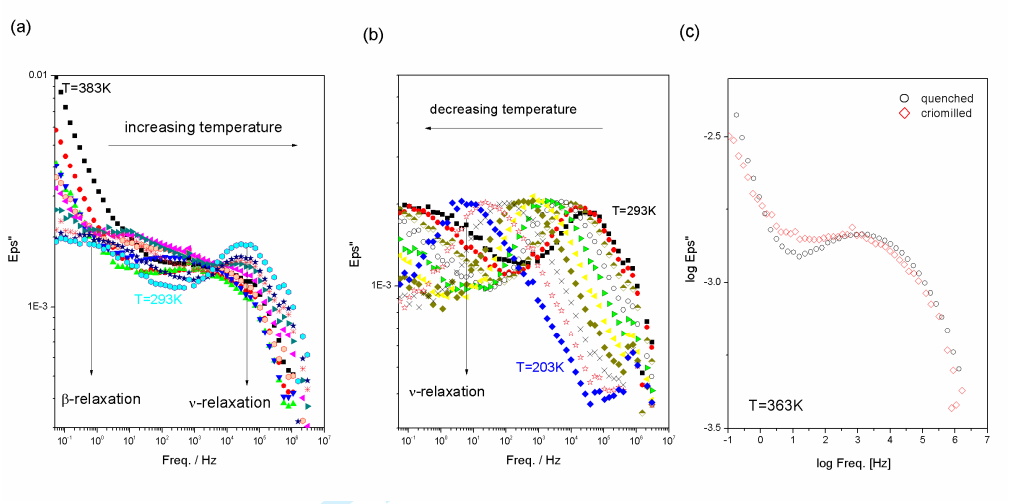

Figure 3. Panels: (a) Dielectric loss spectra in the amorphous state of cryomilled TEL measured from 293K to 383K in step of 10K (b) Dielectric loss spectra in the amorphous state of cryomilled TEL measured from 293K to 203K in step of 10K (c) Comparison of dielectric spectra collected below T_g (at T=363K) for TEL samples obtained using various method of amorphization: quenching and cryomilling.

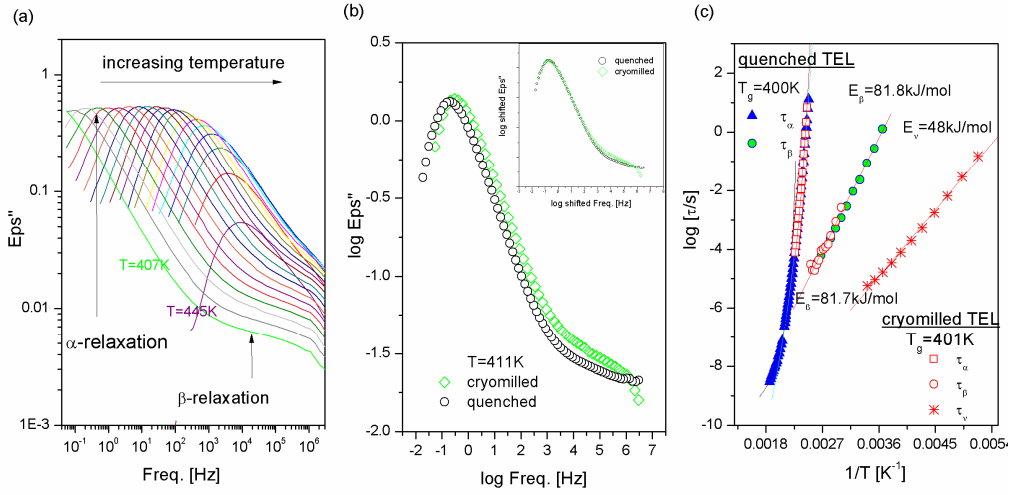

Figure 4. (a) Dielectric loss spectra for cryomilled TEL collected above T_g in step of 2K. (b) Comparison of dielectric loss spectra for quenched and cryomilled TEL at 411K. The inset presents the same data in double logarithmic scale horizontally shifted to superimpose. (c) Relaxation map of quenched and cryomilled TEL. Blue solid triangles and green circles denote structural and β- relaxation times quenched sample. The temperature dependences of α and β-relaxation times for quenched sample originated from our previous studies [35]. Red open squares, circles and stars are respectively α, β and ν-relaxation times of cryomilled sample. Solid lines are VFT and Arrhenius fits to the temperature dependences of the structural and secondary relaxation times, respectively.

Deleted: 30

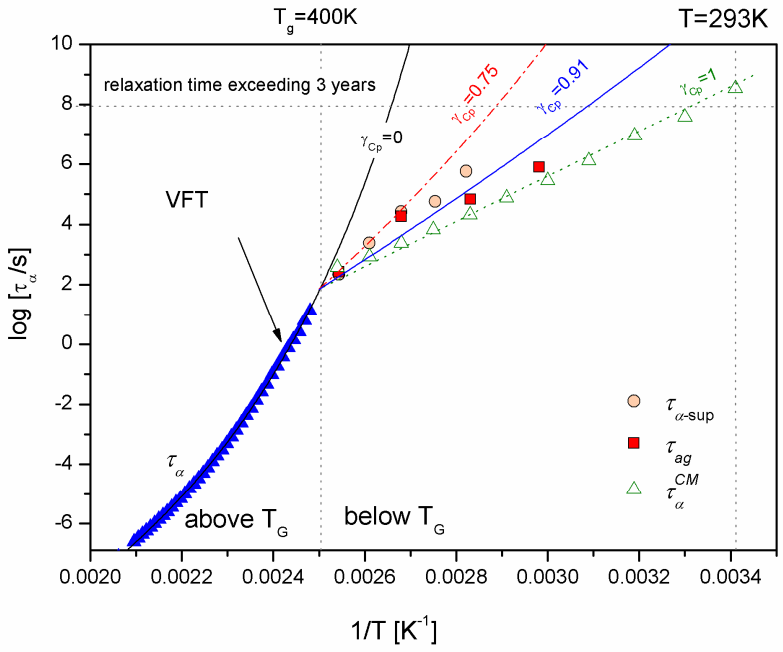

Figure 5. Structural relaxation behavior of TEL above and below T_g. Temperature dependence of τ_α above T_g revealed VFT-like behaviour [35]. In the glassy state, structural relaxation times were evaluated in various different ways i.e. by following β-relaxation changes while aging experiment (red squares - τ_{ag} [35]), by horizontal shift of the α-peak from the region above T_g to the temperatures below T_g (yellow circles - $\tau_{\alpha-\mathrm{sup}}$ [35]), from the Coupling Model (open triangles - τ_α^{CM} [36]). These data were taken to predict structural relaxation behavior based on AGV equation. For structural relaxation times τ_α^{CM} we get Arrhenius-like behavior, $\gamma_{C_p}=1$ (green dotted line), while for τ_{ag} and $\tau_{\alpha-\mathrm{sup}}$ almost Arrhenius-like dependence, $\gamma_{C_p}=0.91$(blue solid line). The structural relaxation times predicted using heat capacities data for a freshly formed glass revealed more VFT-like dependence and are shown as a red dash-dotted line with $\gamma_{C_p}=0.75$.

Deleted: 30

Deleted: 30

Deleted: 30

Deleted: 31

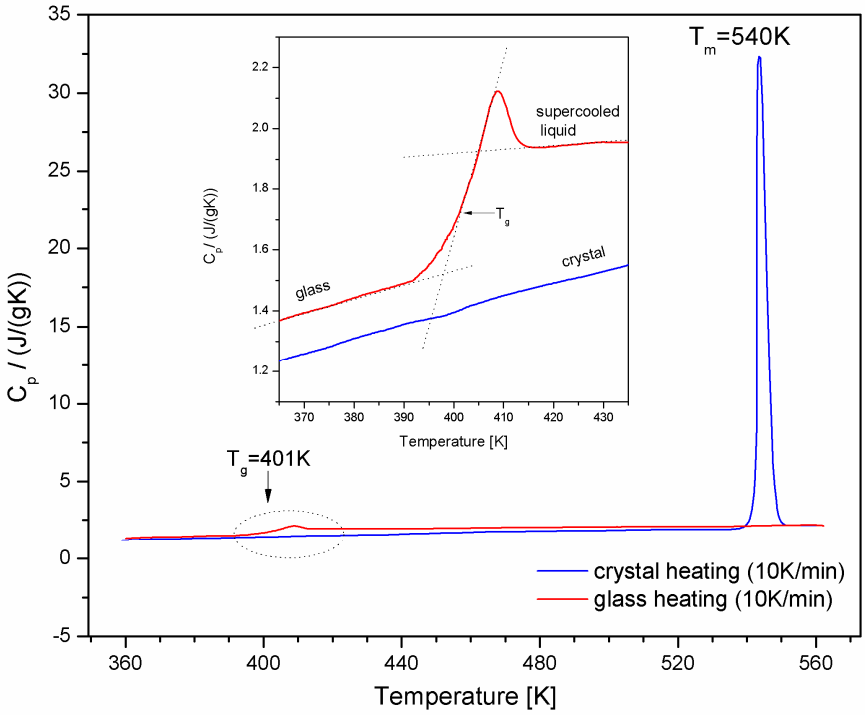

Figure 6. Typical heat capacity profile for crystalline (blue curve) and amorphous TEL (red curve). The heat capacity data were recorded during heating crystalline TEL from 360K to above its melting point T_m=540K. After melting the sample was cooled as fast as possible in order to its vitrification. Subsequently heated amorphous TEL revealed the glass transition temperature at 401K. At higher temperatures there is no evidence of re-crystallization. The inset enlarges the glass transition region obtained on heating.

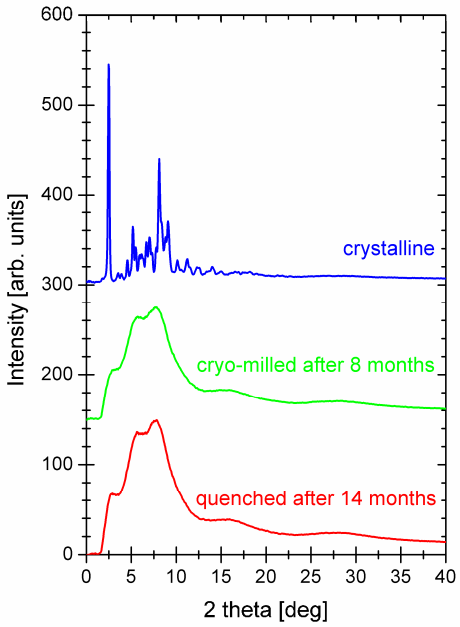

Figure 7. The X-ray diffraction patterns of TEL recorded at room temperature. Panels correspond to: (a) crystalline TEL, (b) cryomilled after 8 months and (c) quenched after 14 months.

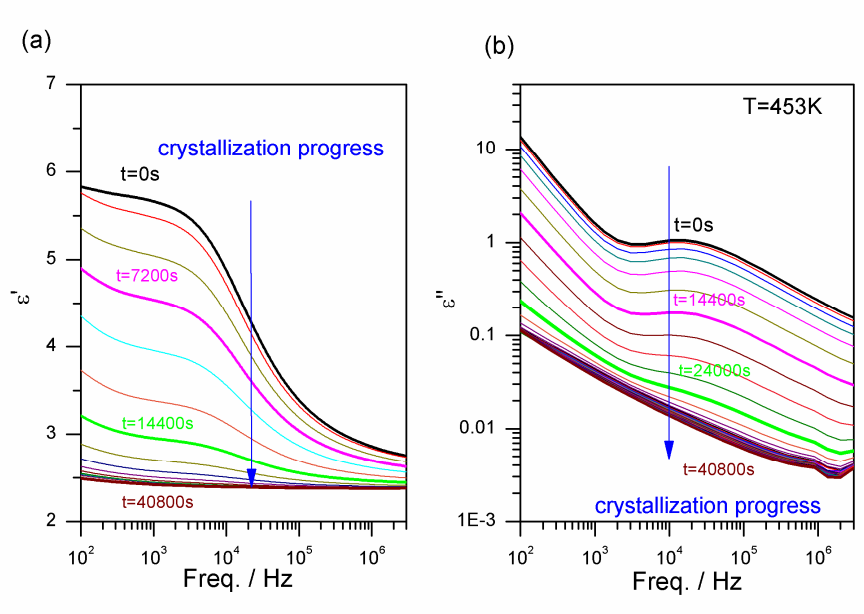

Figure 8. Time evolution of the real (panel a) and imaginary (panel b) part of complex dielectric permittivity plotted versus frequency during crystallization at T=453K.

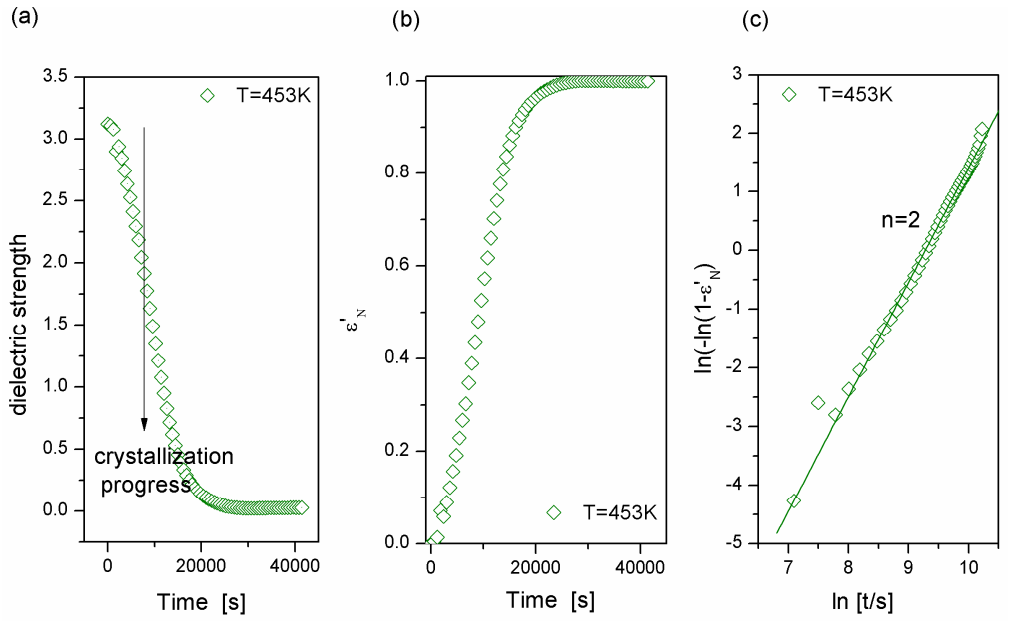

Figure 9. Typical DS profiles for isothermal crystallization of TEL at T=453K:

(a) time evolution of dielectric strength Δε during crystallization progress

(b) normalized dielectric constant ε'_N as a function of crystallization time

(c) Avrami plot

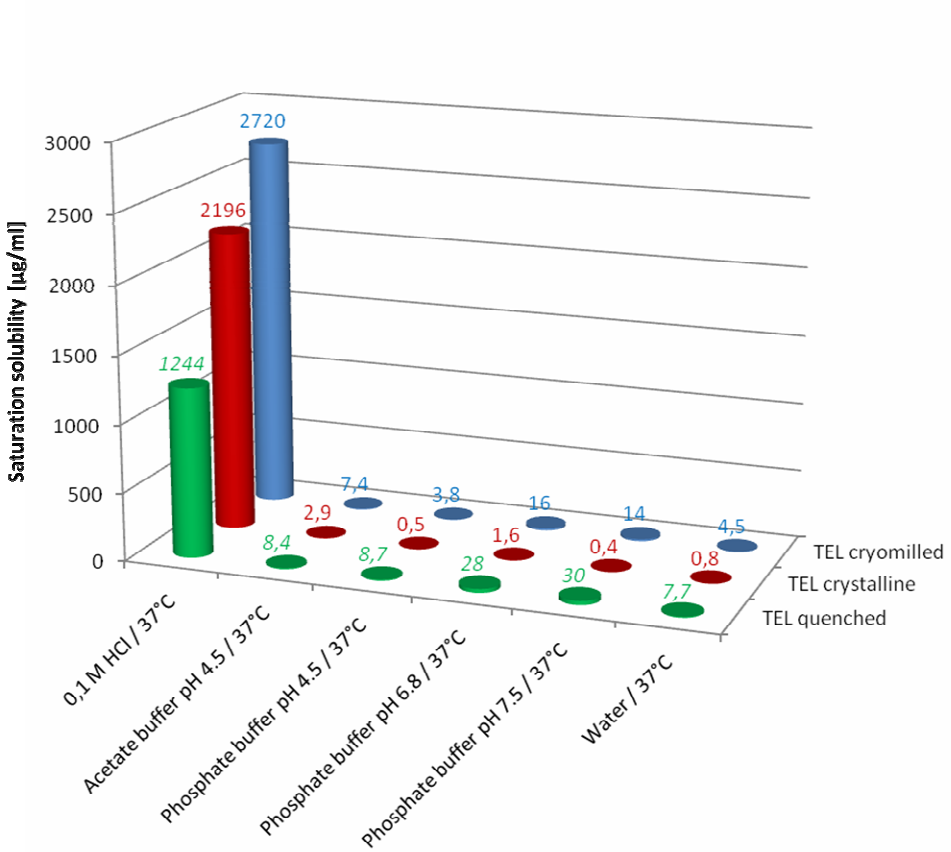

Figure 10. Comparison of saturated solubility of crystalline, cryomilled and quenched TEL samples in different mediums at 37°C.

Table I. Comparison of impurities profile of different forms of telmisartan

Analyte identification	**Relative retention time**	**telmisartan crystalline**	**telmisartan amorphous (cryomilled)**	**telmisartan amorphous (quenched)**
		Amount of analyte [%]		
impurity 01	0.17	-	0.09	0.11
impurity 02	0.73	-	-	0.03
impurity 03	0.76	0.02	0.03	0.03
impurity 04	0.87	-	-	0.03
impurity 05	0.88	-	0.03	0.03
impurity 06	0.97	0.02	0.03	0.06
Telmisartan	**1.00**	**99.96**	**99.80**	**99.49**
impurity 07	1.17	-	-	0.04
impurity 08	1.25	-	-	0.05
impurity 09	1.31	-	0.02	0.09
impurity 10	1.35	-	-	0.02
impurity 11	1.43	-	-	0.02
		Total impurities **0.04**	Total impurities ***0.20***	Total impurities ***0.51***

Table II. Saturated solubility of telmisartan in different medias

Media	Temperature	Saturation solubility [µg/ml]		
		Telmisartan crystalline	Telmisartan cryomilled	Telmisartan quenched
0.1 M HCl	37°C	2196	2720	1244
Acetate buffer pH 4.5		2,9	7,4	8,4
Phosphate buffer pH 4.5		0,5	3,8	8,7
Phosphate buffer pH 6.8		1,6	16	28
Water		0,4	14	30
Phosphate buffer pH 7.5		0,8	4,5	7,7